

pubs.acs.org/Macromolecules Article

Evolution of Chain Dynamics and Oxidation States with Increasing Chain Length for a Donor-Acceptor-Conjugated Oligomer Series

Saadia Chaudhry, Yukun Wu, Zhiqiang Cao, Shi Li, Jodie L. Canada, Xiaodan Gu, Chad Risko,* and Jianguo Mei*



Cite This: https://doi.org/10.1021/acs.macromol.1c00963



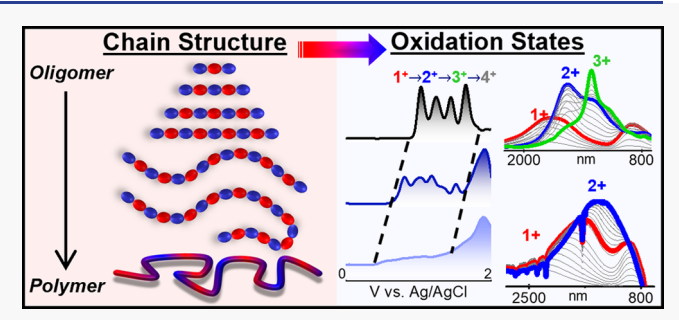
ACCESS

III Metrics & More

Article Recommendations

s Supporting Information

ABSTRACT: While it is known that the chain length strongly affects the properties of π -conjugated polymers, the effects of chain length on the molecular structure, chain conformation, and oxidation state properties in donor—acceptor-type conjugated structures remain unclear. This limits our understanding of how the polymer molecular weight impacts material properties. Here, a discrete and monodisperse oligomer series (n = 3, 5, 7, 9, 15, and 21) and polymers (nPB), composed of the donor 3,4-propylenedioxythiophene (ProDOT), the acceptor benzothiadiazole (BTD), and methylthio end-capping groups, are synthesized by C-H-activated cross-coupling. The molecular structure,



molecular weight, and dispersity of each oligomer/polymer are thoroughly characterized by nuclear magnetic resonance spectroscopy, mass spectrometry, and gel permeation chromatography. This series reveals a rod-to-coil transition at n = 15 and coil formation at polymer length scales of ~28 units via solution small-angle neutron scattering characterization. The oxidation states are deciphered via cyclic voltammetry, differential pulse voltammetry, spectroelectrochemistry, and density functional theory calculations. Oligomers 3–9 undergo successive one-electron oxidation steps, while 15 and higher undergo multielectron oxidations per step in CH_2Cl_2 —TBAPF₆ at a Pt ultramicroelectrode. The electronic transition of each oxidation state (1+, 2+, 3+, etc.) is tracked by absorption spectroscopy, revealing a "bipolaron to di-polaron" transition at n = 7 at which shorter oligomers prefer bipolaron formation and longer oligomers prefer di-polaron formation in their dication states. Furthermore, oxidized 15 has a lower electronic transition energy compared to its polymer homologue, as shown by spectroelectrochemistry, revealing a synergy between the chain length and the oxidation state properties. This study proves that the convergence limit between small molecule and polymer behavior occurs at approximately 15 units and highlights the property transitions that occur as a function of chain length for a donor—acceptor class of conjugated organic materials.

INTRODUCTION

 π -Conjugated polymers (CPs) can be used to develop multifunctional materials whose electrical and mechanical properties are linked to not only the chemical make-up and electronic structure of the π -conjugated backbones but also the chain-length-dependent conformations of these semiflexible, often disordered chains. 1 Most CP-based materials are practically amorphous and can be made conductive by doping (oxidation or reduction).² Alkylenedioxythiophenes, particularly 3,4-propylenedioxythiophene (ProDOT),-based polymers are a unique class of p-type materials developed by Reynolds and co-workers that exhibit strong electron donor effects, moderate band gap energy, and exceptional redox properties.^{3–9} Discovery of these properties has encouraged the development of ProDOT-based CPs specifically tailored for applications in non-linear optics, 10 transistors, 2 batteries, 11-15 photovoltaics, ¹⁶ sensors, ^{17,18} and electrochromics. ³⁻⁹ One of the simplest ways to take advantage of the strong electron-rich properties of ProDOT is to couple it with electron-poor

monomers to construct donor—acceptor (D—A)-type structures.³ Control of the monomers' electron donor and acceptor strength, monomer ratio, and sequence allows fine regulation of the polymer's electronic properties and thereby control of the materials' optical and electronic properties. While the device properties of D—A CPs have been well characterized for a variety of structures, our current understanding of how the chain length affects the chain structure and redox properties of D—A CP systems is limited^{19–21} and requires investigation.

Considering that the redox-active optical and electronic properties of CPs are controlled by the structural features of a polymer chain, primarily the molecular structure, chain length,

Received: May 3, 2021 Revised: August 11, 2021



Scheme 1. Structure of nPB Series: n = 3, 5, 7, 9, 15, 21 and Polymers P1, P2, and P3 Composed of the Monomers Propylenedioxythiophene (ProDOT) and Benzothiadiazole (BTD)

nPB Series

and spatial conformation over multiple length scales,²² it is important to understand how the backbone conformation evolves with the chain length. The intrinsic nature of the CP backbone is determined by the dihedral (torsion) angle potential among the monomer units, steric hindrance from the alkyl side chains, and the chain length. The overall shape of the polymer backbone is dictated by the ratio between the persistence length (Lp), or the rigidity of the conjugated backbone, and the contour length (L_c) , or the end-to-end distance of a stretched-out polymer chain. If L_p is significantly larger than L_{o} the chain behaves like a rigid rod. When L_{p} is comparable to L_{ct} the chain behaves as a semiflexible chain. However, if L_p is significantly shorter than L_c at long lengths, the chain becomes a flexible coil. Only a few polymers are extremely stiff, such as DNA (persistence lengths, 50-70 nm). 23,24 Despite the stiffness of DNA, it behaves as a flexible coil if it is long enough. CPs cannot achieve the same persistence lengths as DNA because of their semiflexible backbones. The CPs poly(3-hexylthiophene) (P3HT) and poly(diketopyrrolopyrrole-thienothiophene) have been observed to have experimental persistence lengths of 3 and 15 nm, respectively.²⁵⁻²⁷ Additionally, their semiflexible, wormlike nature leads to conformational disorder and hierarchical structures across multiple length scales, giving rise to a complex doping/charge behavior in polarons (radical cations), bipolarons (dications), and di-polarons (two radical cations).^{1,28} Considerable effort has been dedicated to determining the relationship between the chain conformation and physical properties of trans polyacetylene, polyaniline, and regioregular P3HT^{29,30} because they can produce highly ordered structures in thin films with well-resolved spectral and crystallographic features. 31-36 Additionally, extensive investigation of their oligomer properties as a function of chain length has led to significant improvement in the design and performance of p-type homo-CP-based electronic devices. 37-40

In contrast to polydisperse polymers, monodisperse oligomers with well-defined molecular structures serve as excellent substitutes for deciphering the behavior of polymers as a function of chain length. 41-44 This is because the chain structure, conformation, and properties of oligomers are easier to characterize by conventional techniques and can be reliably used to extrapolate chain-length-dependent polymer properties. Important features concerning the electronic structure and charge behaviors 45-48 of CPs have been revealed by this approach including charge delocalization (polaron-bipolaron model),^{36,49–52} interactions of radical spins,^{53–56} exciton dynamics, 53-56 and effective conjugation lengths 57-63 for electron-rich homo-oligomers such as oligo-thiophenes, 64-71 -phenylenes,⁷² -phenyl ethylenes,^{73,74} -vinylenes,^{75,76} -acetylenes,^{77,78} and -fluorenes.^{79,80} Compilation of these studies has allowed the establishment of several redox trends for conjugated systems as a function of increasing chain length, including (i) an increase in the number of redox states, (ii) a decrease in the oxidation potential, (iii) a decrease in the potential difference between subsequent redox states, (iv) separation of multiple charges within a chain due to Coulombic repulsion, and (v) an increase in chemical stability of the charged species. In contrast to donor-only systems, only a few reports have investigated the chain-length dependence of alternating D-A conjugated oligomers, 19-21 whereas most D-A-focused studies have explored the influence of the monomer sequence^{55,81-83} and the electron-withdrawing strength of the acceptor unit. 84–86 Considering the importance of low band gap, D-A-type structures in organic electronic devices, it is of great interest to explore how the chain length, conformation, and charged states govern their optical and electronic

Herein, we report the impact of increasing chain length on the chain conformation and redox-active optoelectronic properties of a conjugated D-A oligomer series ranging from n = 3 to 21 and polymers (nPB). Composed of the D unit ProDOT and the A unit benzothiadiazole (BTD), as

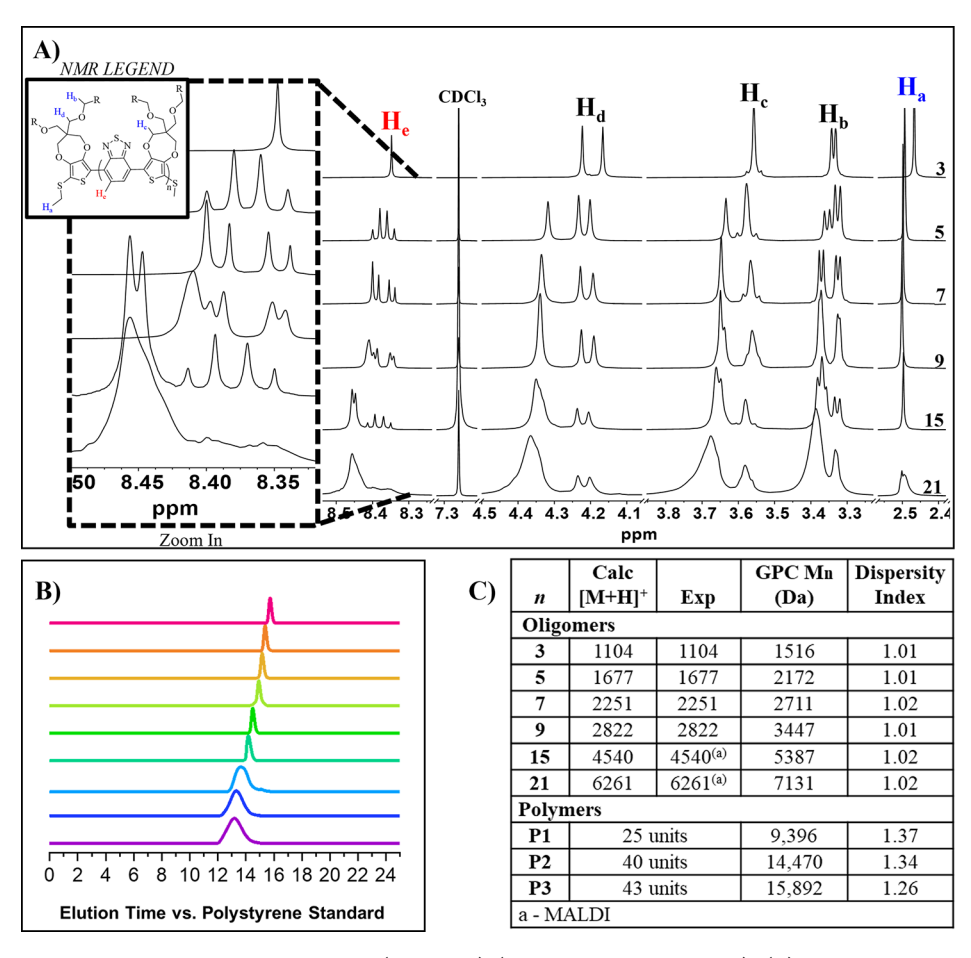


Figure 1. (A) ¹H NMR spectra of the *n***PB** series in CDCl₃ (7.26 ppm) (inset: proton peak legend). (B) Gel permeation chromatograms of the *n***PB** series. (C) Summary of GPC and HRMS analysis data of the *n***PB** series.

shown in Scheme 1, this model oligomer series is used to uncover the correlation between the chain conformation, oxidation properties, and the resulting optical and electronic features. Additionally, this oligomer series is used to extrapolate and decipher the properties of their D–A polymer homologues *via* their underlying mass scaling relationship.

■ RESULTS AND DISCUSSION

The direct acquisition of various oligomer lengths by stepwise and iterative palladium-catalyzed carbon-carbon (C-H/C-Br) coupling of the ProDOT and BTD monomers allowed us to construct a complete series of monodisperse conjugated oligomers and their polymer homologues with increasing chain length. A segmented synthetic procedure was used where oligomers of known lengths are added to the end(s) of another oligomer chain with subsequent purification and chain-end functionalization. This allowed the oligomer chains to grow by several units per iteration, in contrast to one-unit growth per iteration. Synthetic and purification procedures of the nPB series are provided in the Supporting Information. We begin the following discussion by first verifying the molecular structure and dispersity of each molecule in the nPB series via NMR spectroscopy and mass spectrometry (MS). Second, we use solution small-angle neutron scattering (SANS) spectroscopy to quantity the relationship between the chain length and conformation through which we identify a "rod-tocoil" conformational transition. Finally, the optical and electronic properties of the oxidation states for each oligomer

and polymer are characterized by density functional theory (DFT) calculations, solution voltammetry, and spectroelectrochemistry.

Molecular Structure. NMR Analysis. Representative ¹H NMR spectra of nPB are shown in Figure 1A. The ratio between the end-capping group methylthio protons (Ha) and the BTD protons on the chain backbone (He) was used to determine the molecular structure of the oligomers. Hb, Hc, and Hd represent the chemical shifts of the propylene bridge and solubilizing alkyl chain protons, as shown in the labeled inset of Figure 1A. The transformation of each proton environment with increasing chain length is described below. In the following text, the prefix "end-" and "mid-" will be used to distinguish between the different location points on the oligomer chain.

Aromatic Protons (Ha and He). As the oligomer chain grows, the ratio of Ha/He increases as 6:2 (3), 6:4 (5), 6:6 (7), 6:8 (9), 6:14 (15), and 6:20 (21). He manifests as a singlet in 3 and doublet-of-doublets (dd) in 5, indicating the non-equivalence of the BTD protons at the end of the chain versus toward the middle of the chain. As the chain length increases from 5 to 7 to 9, two different He environments emerge composed of a singlet overlapping with the dd peak. The dd peak is representative of the end-BTD protons, and the singlet peak is representative of the mid-BTD protons. With the continuing increase in the chain length to 15, a new proton environment for the mid-BTD He protons is observed. This peak broadens and is no longer resolvable at n = 21, as is

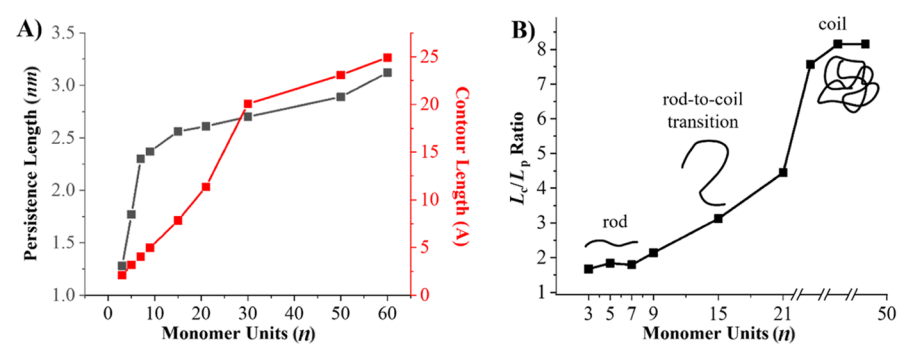


Figure 2. (A) Persistence length of *n*PB oligomers and polymers with different numbers of repeating units fitted by a flexible cylinder model in SasView. (B) L_c/L_p change with the number of repeat units.

typically observed for polymers at room-temperature NMR time scales. Furthermore, the steady downfield chemical shift of the He mid-chain protons saturates at 21, indicating an increase in aromaticity in the conjugated backbone from 3 to 21 units.

The ¹H NMR spectra of the polymer samples exhibit similar features as n = 21, although with broader peaks. End-group analysis of the He/Ha peak ratio was used to calculate the molecular weight of P1, P2, and P3 as 25, 40, and 43 units, respectively (deconvoluted and integrated NMR spectra are shown in the Supporting Information). This result was verified by gel permeation chromatography (GPC), as discussed in the following section. As the molecular weight increases, peak broadening diminishes the resolution between the end-chain and mid-chain proton environments, although the difference is still notable.

Alkyl Protons (Hb, Hc, and Hd). These peaks represent the propylene bridge protons and the chiral alkyl chain. The presence of the alkyl-solubilizing chain creates a center of chirality at the C2 position of the propylene bridge, giving rise to two distinct stereoisomers of the monomer. The Hb peak of the alkyl chain is split into a doublet due to its presence near a chiral center. As the chain grows larger than 3, this single doublet is split into double doublets, with an upfield doublet representing the end-ProDOT units and retaining a constant integral value and chemical shift with increasing chain length. The downfield doublet is characteristic of the mid-ProDOT units in the chain and hence increases in ratio as the chain length grows. The same trend is seen for the Hc and Hd proton environments, where the end-ProDOT monomers are detected to have a distinct chemical shift from the rest of the D units in the oligomer chains. Eventually, resolution is lost at 21 units as was the case for the aromatic protons. Nonetheless, the two environments of the end-ProDOTs versus the mid-ProDOTs can be differentiated, even for the polymers. The rest of the alkyl chain protons are detected between 1.8 and 0.8 ppm and are shown in the Supporting Information.

Mass Analysis. The nPB series was evaluated by GPC, atmospheric pressure chemical ionization (APCI) MS, and matrix-assisted laser desorption ionization (MALDI) MS to confirm the molecular weight and dispersity. The gel permeation chromatograms of sample refractive index versus time are shown in Figure 1B. The series follows a linear trend where 3 has the lowest molecular weight and the highest elution time and 21 has the highest molecular weight and the lowest elution time. More importantly, all oligomers possess close to perfect monodispersity at a PDI value of $1.01 \, (\pm 0.01)$. As the oligomer chain grows from 3 to 21 units, the accuracy

of the $M_{\rm n}$ values determined by GPC increased. High-resolution MS (HRMS) was conducted to verify the molecular weight of each oligomer and the accuracy of the GPC results. These results are further supported by NMR characterization, giving us confidence on the monodispersity and molecular structure of each species in the series. The calculated and experimental mass analyses are summarized in Figure 1C.

Chain Conformation. *Solution-Phase Small-Angle Neu*tron Scattering Analysis. Solution SANS is a well-established method to measure the chain conformation of polymeric chains in a dilute solution. The neutron scattering contrast arises from the scattering length density difference between the hydrogenous D-A CPs and the deuterated solvent. Representative SANS curves of the nPB oligomers and polymers are shown in Supporting Information, Figure S9. The scattering profiles show drastic increases in low q intensity as the molecular weight increases, as low q scattering is very sensitive to large structures in solution. The polymer backbone rigidity is related to $L_{\rm p}$, the characteristic length scale at which the chain begins to bend more than 90° along the backbone direction. Potential molecular or chain aggregation was avoided by the solvent choice and elevated temperatures to fully dissolve the oligomers/polymers. Additionally, the sample was measured at low concentrations to relate the measured scattering data to the form factor of each oligomer/polymer. In the present work, we measured our samples at 75 °C in deuterated chlorobenzene. To acquire the quantitative comparison of conformational characteristics, the SANS data were fitted using a flexible cylinder model in SasView software to extract the contour length, persistence length, and radius for each sample. Details on the flexible cylinder model can be found here.³⁰ As shown in Figure 2A, the contour length, a parameter that measures the longest possible chain conformation, increases from 2.1 nm for 3 to 24.9 nm for P3, which is in reasonable agreement with the predicted backbone length based on the measured molecular weight. Remarkably, $L_{\rm p}$ only increases from 1.28 to 3.12 nm. It is worth noting that L_p quickly increases from 3 to 7 and then plateaus until it stabilizes at about 3 nm for the polymers. Furthermore, the acquired persistence length of the entire polymer is close to the chain rigidity for P3HT, as determined by Segalman et al.²⁷ It was observed that P3HT also has a persistence length of 3 nm. This similarity between the backbone rigidity of the homopolymer P3HT and alternating D-A poly(ProDOT-BTD), P1-P3, suggests that the alternating co-thiophene structure and the non-alternating homo-thiophene structure experience a similar amount of backbone torsion.

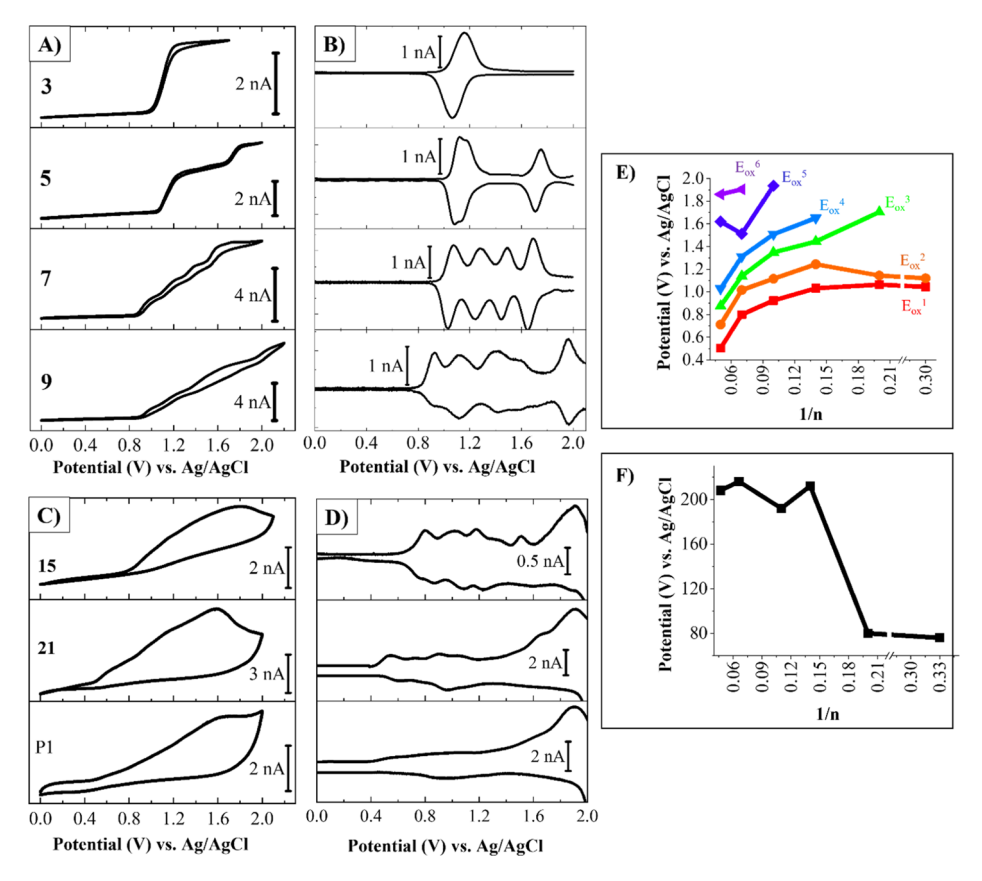


Figure 3. Electrochemistry of D–A series at 1 mM analyte concentration in 0.2 M TBAPF $_6$ /CH $_2$ Cl $_2$ at a 25 μ m Pt UME ν s Ag/AgCl. (A) CV curves at 10 mV/s for 3, 5, 7, and 9, (B) DPV curves for 3, 5, 7, and 9, (C) CV curves at 10 mV/s for 15, 21, and P1, (D) DPV curves for 15, 21, and P1, (E) anodic potentials of all oxidation states as a function of chain length, and (F) anodic potential difference between the first and second oxidation peaks as a function of chain length.

To explore the shape of CP chains, the ratio between L_c and L_{p} was calculated and plotted against molecular weight, as shown in Figure 2B. Overall, three regions can be identified in the curve. For low-molecular-weight oligomers (below 9 units), the ratio of L_c to L_p is around 2, corresponding to a semiflexible worm-like chain. This means that even shorter oligomer chains are not entirely rigid, which can be attributed to the backbone torsion from the alternating D-A backbone. For high-molecular-weight polymers (P2 and P3), the ratio of L_c to L_p increases to 8, meaning that the polymer chain behaves like a flexible coil shape, which is reasonable for a long chain. Concurrently, 15 falls within the range at which a rodto-coil transition occurs for the nPB series, marking the distinction between oligomer and polymer chain properties. The electronic consequences of this chain-length-dependent transition are explored via electrochemistry and UV/vis spectroscopy as described below.

Oxidation Characteristics. *DFT Calculations.* In this section, we turn our attention toward understanding how the elongation from oligomer to polymer length scales impacts the redox and optical properties of a conjugated D–A system. We begin this analysis with DFT calculations of varied charged states of n = 3, 5, 7, 9, 15, and 19; in addition to the neutral electronic state, the +1 (doublet, n = 3-19), +2 (singlet and triplet, n = 3-9), +3 (doublet and quartet, n = 5-9), and +4 (singlet, triplet, and quintet, n = 5-9) charged (spin) states were considered. We note that we were not able to achieve a converged radical-cation state for 21 and so this structure is not included in the computational analyses. The calculations

were performed at the OT- ω B97X-D/6-31G(d,p) (OT = optimally tuned) level of theory, $^{87-89}$ where the range-separation parameter ω for each molecule was tuned via the ionization-potential-tuning procedure. All alkyl chains were truncated to methyl groups to reduce the computational cost, and each optimized geometry was confirmed as a minimum on the potential energy surface through normal mode analysis. The influence of the solvent environment (CH₂Cl₂; $\varepsilon=8.93$) was modeled using the polarizable continuum model. The Gaussian 09 software suite was used for all DFT calculations. The relative energies of each spin state for each oxidation state are given in the Supporting Information.

The computed adiabatic ionization potential for n = 3-19 follows 5.23 eV (3), 5.00 eV (5), 4.88 eV (7), 4.84 eV (9), 4.82 eV (15), and 4.82 eV (19). These trends suggest that the effective conjugation length $^{50,63,94-97}$ for this D–A system is reached at approximately 9 units. For 3, 5, 7, and 9, a broken symmetry radical-cation state is the most stable conformation by 96, 70, 34, and 12 meV, respectively; this broken symmetry state is achieved by the rotation of one of the end-cap methyl thiol moieties with the charge localizing on one end of the molecular structure. The situation is reminiscent of a Robin and Day Class II mixed-valence system. For 15 (and 19), the symmetric configuration of these moieties is the most favorable, with the charge localized closer to the center of the molecular structure; in both instances, the symmetric structure is energetically favorable by \sim 40 meV. Plots showcasing the bond length alternation patterns of these

Table 1. Summary of Anodic Potentials of nPB (3 to 21 and P1) via DPV in 0.2 M TBPAF₆-CH₂Cl₂ at ~1.0 mM

n	$E_{ m pa}^{-1}$	${E_{\mathrm{pa}}}^2$	$E_{ m pa}^{-3}$	$E_{ m pa}^{-4}$	$E_{ m pa}^{-5}$	$E_{ m pa}^{}$
3	1.044 (1e) ^a	1.120 (1e) ^a				
5	$1.064 (1e)^a$	1.144 (1e) ^a	1.704 (1e)			
7	1.032 (1e)	1.244 (1e)	1.444 (1e)	1.652 (1e)		
9	0.924 (1e)	1.116 (1e)	1.348 (1e)	1.508 (1e)	1.936 (1e)	
15	0.800	1.016	1.140	1.311 ^a	1.512	1.904 (ne)
21	0.504	0.712	0.876	1.028	1.620	1.860 (ne)
P1	~0.4 (onset of oxidation)					

^aCalculated from deconvoluted data. Note: 1e = ~1 nA current magnitude by DPV at 1.0 mM concentration.

varied states versus the respective neutral states are given in the Supporting Information.

Moving to the +2 charge in n = 3-9, the singlet state is more energetically stable in 3 and 5, which suggests that bipolaron (i.e., spin-paired dication) formation is preferred. This preference suggests that the energy gained by forming a single structural deformation through the bipolaron outweighs the increased Coulomb repulsion energy from two separate charges. 92 However, for the longer systems 7 and 9, it is the triplet state that is more energetically favorable, suggesting that two independent polarons (i.e., spin-unpaired dication) are present. These results demonstrate the length dependence concerning the preferred formation of a bipolaron or two polarons, 92 and an interplay between energy (de)stabilization due to electron pairing and Coulombic effects. For the +3 charge, the doublet state is more energetically stable in every case examined. The +4 charge is somewhat more complicated in terms of the preferred spin state: in 5 and 9, the order follows singlet, triplet, and quintet, while in 7 it follows triplet, singlet, and quintet. Note that we treat the results of these higher-charged states with caution because several effects could potentially stabilize one state (e.g., polaron vs bipolaron formation) over another in the experiment—including explicit interactions with solvent molecules and/or counterions—not accounted for in the DFT calculations. Plots of the relative energies of these different charged states are provided in the Supporting Information.

Voltammetry. With this understanding of, albeit isolated, oligomers in hand, we turn to electrochemical studies. The voltammetry of CPs, typically conducted in the solid state, is plagued with non-Faradaic effects such as the capacitance, film resistivity, lattice expansion, and contraction effects, resulting in broad and ill-resolved voltammetric waves. Additionally, cyclic voltammetry (CV) experiments of CPs contain both kinetic (scan rate) and thermodynamic data ($E_{1/2}$ potential), making it difficult to separate the different energetic effects. Therefore, the potential and shape of voltammetric waves determined as a function of molecular length for discrete and well-defined oligomers can provide an insight into understanding the electron-transfer mechanisms, structural changes, and charge interactions of their polymer homologues. To determine the electrochemical oxidation processes for the *n*PB series, solution electrochemistry via CV and differential pulse voltammetry (DPV) was studied in 0.2 M TBAPF₆-CH₂Cl₂ on a 25 μ m Pt ultramicroelectrode (UME) surface. The CV and DPV voltammograms are shown in Figure 3A-D, and the electrochemical data are summarized in Table 1.

The use of a UME for macromolecular electrochemistry in solution is advantageous because it overcomes slow mass transport, large double-layer capacitance, and large Ohmic loss, typically experienced on macroelectrode surfaces. $^{99-101}$ This

can be achieved under steady-state mass transport conditions, in which the electrolysis rate is approximately equal to the rate of (radial) molecular diffusion at the surface of the electrode, causing the product of electron transfer to diffuse away from the electrode and is the reason why no peak is observed on the reverse CV scan. If steady-state conditions are not met, then the electron-transfer product that is formed on the forward part of the voltage scan does not have sufficient time to diffuse away from the electrode surface and so it is converted back to the neutral state on the reverse scan, hence increasing the area between the forward and reverse scans. Deviation from ideal steady-state conditions for the nPB series becomes apparent at the 9 unit chain length, as shown in Figure 3A, where the area between the forward and reverse scans begins to increase. Deviation from steady-state conditions is more pronounced in 15, 21, and P1, where the previously mentioned advantages of using a UME for CV are diminished. An increase in the molecular size, an increase in the number of electron-transfer steps with similar ionization energies, and a change in diffusion coefficients at longer chain lengths all contribute to slow mass transport, high double-layer charging currents, and shifts in iR drop to distort the current-voltage voltammograms of 15, 21, and P1 from ideal behavior. Keeping the CV parameters for all oligomers and polymer samples constant allowed us to reveal the impact of the chain length on the steady-state conditions for the *n*PB series. It should be noted that attempts to find the steady-state conditions for longer systems at slower scan rates had a low signal-to-noise ratio and faster scan rates caused higher double-layer charging currents during CV. We chose to overcome this problem by performing DPV, which proves the reversibility of all the oligomers and polymers. DPV allowed minimization of the double layer capacitance effects and maximization of the Faradaic response, especially for the longer systems. The electrochemical reversibility of 9, 15, 21, and P1 is also observed during spectroelectrochemistry, discussed in the next section, by change in solution color from the visible neutral state to the transmissive oxidized state and back to the visible neutral state.

As previously reported, 102 3 exhibited two successive anodic peaks appearing at $E_{1/2}=1.044~\rm V$ versus Ag/AgCl with a very small potential difference ($\Delta E_{1/2}^{1-2}$) of 76 mV and net chemical reversibility. The seemingly single anodic peak was resolved by deconvolution to reveal two separate peaks (Figure S5 in the Supporting Information). This result suggests that the dication forms immediately after the radical cation. The first anodic potential for 5 occurs at $E_{1/2}=1.064~\rm V$ versus Ag/AgCl, 20 mV higher than 3. An increase in the oxidation potential with an increase in the conjugation length was unexpected, as similar π -conjugated systems undergo a decrease in the oxidation potential with increasing chain length. This deviation from the expected linear trend was

Table 2. Photophysical Properties (λ_{max}) of the Neutral and Oxidation States of the nPB Series by Spectroelectrochemistry in Solution.

n	$L_{\rm p}$ (nm)	neutral (eV, nm)		+1 (eV, nm)		+2 (eV, nm)		
3	1.28	2.54	489	1.53/0.96	808/1295	2.00	620	
5	1.77	2.28	544	$NR/0.89-0.77^{b}$	NR/1400-1600	1.18/1.04	1052/1191	
7	2.30	2.18	568	1.38/0.70	900/1780	0.80	1553	
9	2.37	2.13	583	1.36/0.63	913/1976	1.30/0.72	952/1729	
15	2.56	2.07	598	$1.36^{b}/0.83-0.44^{b}$	914/1500-280	$1.38/0.72/0.52-0.44^{b}$	900/1722/2400-2800	
21	2.61	2.00	620	$1.33^{b}/0.61$	930/2023	1.27/0.77	980/1620	
P1	2.70	1.95	636	1.23/0.73	1008/1696	0.86	1450	
P2	2.89	1.95	637					
Р3	3.12	1.95	636					

^aValues for the +3 and +4 oxidation states are provided in the Supporting Information. ^bBroad, NR = not resolvable.

attributed to the increase in the acceptor/donor ratio, which is 0.3 for 3, 0.4 for 5, and >0.4 for the longer systems gradually approaching the 0.5 limit for the polymer. Additionally, aggregation or solvation effects 103,104 may be contributing to this behavior as well because crystallite formation was observed for 5 in solution by atomic force microscopy (AFM) (Figure S8 in the Supporting Information). 5 shows three reversible oxidation states, with $\Delta E_{1/2}^{\ \ 1-2}$ equal to 80 mV. Furthermore, oxidation of 5 to the trication state requires a great deal of energy, with $\Delta E_{1/2}^{\ \ 2-3}$ equal to 562 mV.

The oxidation potential of conjugated oligomers and polymers decreases with an increase in the chain length until the effective conjugation length is reached. 63,95,96 In contrast to the shorter oligomers, 7 and 9 follow this trend and show their one-electron oxidation $E_{1/2}$ potentials at 1.032 and 0.924 V versus Ag/AgCl, respectively. For 7, four consecutive oneelectron oxidation peaks with a potential difference of ~200 mV between each state were detected by CV and DPV. This substantial increase in $\Delta E_{1/2}^{1-2}$ indicates Coulombic repulsion between two charges in the dication state. In agreement with the DFT calculations, the di-polaron is more energetically favorable for 7, suggesting the formation of two polarons confined to a single chain instead of a bipolaron. Notably, this result signifies that at a 7-unit chain length, there is a fundamental change in the way the electrons are populated across the conjugated system for the nPB series. Furthermore, oxidation to the 3+ and 4+ states also requires ~200 mV per oxidation step. For 9, five consecutive one-electron oxidation peaks are detected with regard to the five donor units in the chain. Similar to 7, $\Delta E_{1/2}^{1-2}$ for 9 is equal to 192 mV and indicates a large Coulombic repulsion for 92+ as would be expected for two separate but interacting positive charges. Furthermore, oxidation of 9 to the 4⁺ and 5⁺ states is summarized in Table 2.

One-electron oxidation of 15 occurs at 0.800 V versus Ag/AgCl. As the conjugation length increases, successive oxidation peaks begin to coalesce and separation between two standard potentials decreases, producing broad CV waves. The merging of separate voltammetric peaks with increasing chain length implies that the Coulombic repulsion between positive charges in the chain is decreasing, in other words, their ionization energies are becoming similar. Additionally, this voltammetric response may also be attributed to changes in the electron-transfer dynamics of larger chains on the electrode's surface. Because the relationship between oligomer chain conformation and voltammetric response (Faradaic and non-Faradaic) is complex, further studies would be required to make a definitive statement. Nonetheless, multiple anodic waves were detectable

by DPV showing six oxidation states for 15, a molecule with eight donor units. The area beneath the last, broad oxidation peak at 1.8 V for 15 is indicative of multiple electron transfers. It should be noted that the electrochemical window for the electrolyte—solvent system was stable up to 2.1 V oxidation, as shown in the Supporting Information. This deviation from the "one-electron oxidation per donor unit" trend at 15 units is an impact of an increase in the chain length and can also be correlated to the rod-to-coil transition occurring at this approximate length. All oxidation steps are found to be reversible or quasi-reversible.

Similar to 15, the CV curve of 21 is broadly shaped with a drastic decrease of 296 mV in the onset of oxidation occurring at 0.504 V versus Ag/AgCl. The redox potentials of other systems, such as oligofluorenes and oligothiophenes, have also exhibited similar behavior, where the oxidation potential continues to decrease past the maximum conjugation length of the system. 105 Typically, a linear relationship between the redox potential and 1/n is justified by particles in onedimensional boxes, but this does not seem to be the case in this study. We hypothesize that the odd CV behavior of 21 may be a result of a change in free energy caused by an increase in positional entropy, as the positive charge can reside at varied positions along the chain. Additionally, backbone conformational changes caused by chain coiling in solution at lengths longer than 15 may affect the electron-transfer dynamics and adsorption effects at the electrode's surfaces. Solvent and counteranion effects cannot be excluded and may have a cumulative impact on the drastic lowering of the oxidation potential after the maximum conjugation length has been reached. Improved resolution of 21 was obtained with differential normal pulse voltammetry (DNPV), showing an asymmetric voltammogram which indicated that the dedoping process is not the same as the doping process and may be accompanied by different structural transformations or chemical changes across the oligomer chain that were not observed for the shorter oligomer chains. Nonetheless, approximately seven anodic peaks were detected for 21 by DNPV after deconvolution (Figure S6 in the Supporting Information) and a final multielectron-transfer step from 1.6 to 1.9 V. This increase in the peak area of the final oxidation steps is also seen in P1, whose DNPV voltammogram shows numerous small peaks followed by one major peak at 1.8 V. For a polymer of ~25 units with 1.2 PDI (P1), it was pleasing to see narrow, defined peaks for a polymer voltammogram that resembled the anodic wave patterns of its shorter, well-defined parents.

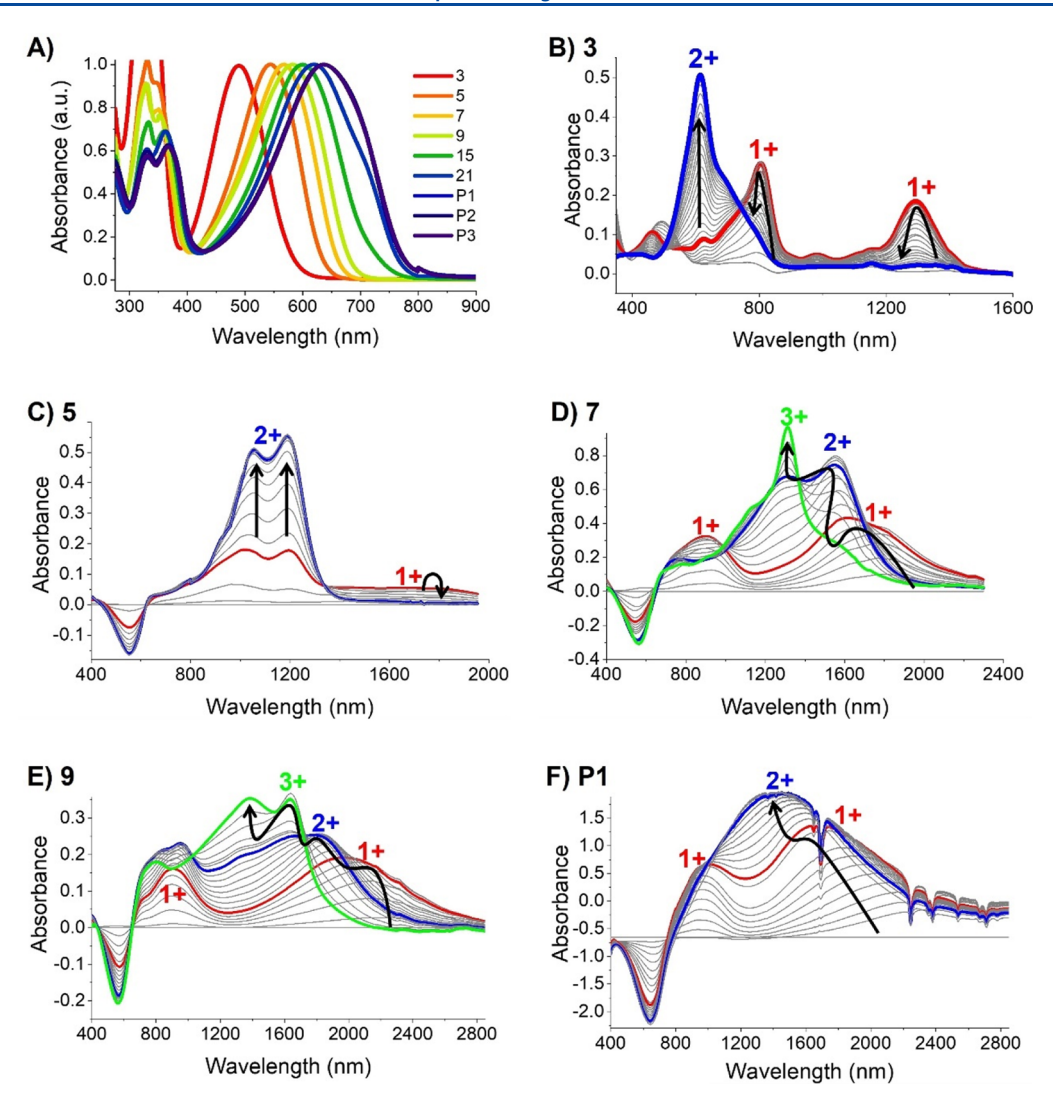


Figure 4. (A) Neutral absorption spectra of *n***PB**. Spectroelectrochemistry results of *n***PB** in 0.2 M TBAPF₆/CH₂Cl₂: (B) 3, (C) 5, (D) 7, (E) 9, and (F) **P1**. This experiment was conducted in an air-tight optically transparent thin-layer quartz cuvette equipped with a Pt honeycomb electrode under nitrogen. The spectra for **15** and **21** are shown in the Supporting Information.

Optical Properties. The absorption spectra of neutral and oxidized nPB in dichloromethane at room temperature are shown in Figure 4 and summarized in Table 2 (eV, nm). All oligomers exhibit the dual absorption band characteristics of D-A systems, consisting of the π -to- π * band and the D-A charge-transfer band. Both peaks bathochromically shift with increasing π -conjugation. An increase in the chain length from n=3 (2.54 eV) to 5 units caused a -0.26 eV bathochromic shift of the D-A band. This change gradually decreased to -0.10 eV from n=5 to 7, -0.05 eV from n=7 to 9, and so forth. The D-A $\lambda_{\rm max}$ increases with increasing chain length and saturates at P1 (~25 units) at a value of 1.95 eV.

Assessment of the neutral absorption properties is confirmed by time-dependent DFT (TDDFT) calculations at the OT- ω B97X-D/6-31G(d,p) level of theory. The S₀ \rightarrow S₁ (π -to- π *) excitation, described in each system as predominately a HOMO \rightarrow LUMO transition (though additional one-electron transitions become important as the oligomer length increases), increases across 3 (2.82 eV), 5 (2.28 eV), 7 (2.11 eV), 9 (2.03 eV), 15 (1.89 eV), and 19 (1.90 eV). We note that, like the ionization potential, the S₀ \rightarrow S₁ excitation

converges at $n \approx 15-19$, suggesting that the effective π -conjugation length has been achieved.

Radical Cation (+1) States. One-electron oxidation of a π conjugated oligomer leads to the formation of a radical cation, otherwise known as a polaron, considered to be a localized charged species with quinoidal and geometrical changes confined to a limited number of monomeric units in a chain. Coupling of the charge with the geometric structure for π conjugated materials causes new electronic states to appear within the band gap of the molecule. For a radical cation, a singly occupied level is generated above the valence band and an empty one appears below the conduction band. 106 In this case, the +1 states of the nPB oligomer series show two major electronic transitions, a high energy and a low energy transition, bathochromically shifted relative to their neutral states. Two high intensity peaks for 3⁺ were found at 1.53/0.96 eV, with weaker mid-gap transitions in between. The radical cation states of the longer oligomers show a continuous bathochromic shift per increasing chain length. The two transitions for 5⁺ were broad and very weak, absorbing approximately at 0.89-0.77 eV. An increase in conjugation to 7^{+} (1.38/0.70 eV) and 9^{+} (1.36/0.63 eV) led to the formation

of strong yet broadly absorbing peaks compared to the shorter chains. At 15⁺ (1.36 and 0.83-0.44 eV) and 21⁺ (1.33 and ~0.61 eV), shown in Figure S7, the isosbestic points became vague as more oxidation states became available, and the ΔE between consecutive oxidation potentials decreased. Additionally, the increase in electronic and vibrational transitions with the increase in chain length and oxidation states makes exact assessment of their spectroelectrochemistry difficult. Nonetheless, partially oxidized 15 absorbs from 0.83 to 0.44 eV nm, and this is the lowest energy transition of all the oxidized states in the entire nPB series. More interestingly, oxidized 21 and P1 (1.23 and 0.73 eV) are hypsochromically shifted to oxidized 15 and so this behavior exhibits an optical saturation and inversion point at the 15-unit chain length. The radical cation transitions for P1⁺ is clear at 1.23 and 0.73 eV, unlike 15 and 21, and falls in the absorption range of 5⁺ and 7⁺ units. This result shows that the oxidation of longer chain lengths does not necessarily produce further NIR-absorbing species, or lower electronic transitions, as one would expect, in comparison to their shorter oligomer counterparts in solution. For all nPB radical cations, the TDDFT calculations show a red shift and an increase in the oscillator strength of the lowest-lying excitation.

Dication (+2) States. Similar to the trend observed for the +1 states of the nPB series, the +2 states undergo bathochromic shifting until the 15-unit chain length. The transition from a radical cation to a dication for 3 is represented by an isosbestic point at 1.69 eV (734 nm) and formation of the dication at 2.0 eV, as previously reported. 102 The dication peak for the nPB series undergoes a bathochromic shift from 2.0 eV for 32+ to 1.18/1.04 eV for 52+, 0.80 eV for 7^{2+} , and 1.30/0.72 eV for 9^{2+} . At chain lengths of 15 and 21, shown in Figure S7, the pure dication states cannot be accurately resolved due to mixing with +1 and +3 states with no clear isosbestic points. Nonetheless, broad absorption peaks at 1.38/0.72/0.52-0.44 eV for oxidized 15 and 1.27/ 0.77 eV for 21²⁺ show that oxidized 15 has the lowest energy transition of all the molecules in the nPB series. This is the same trend observed for the radical cations, as described earlier. P12+ exhibits a very broad and single absorption band at 0.86 eV, as typically seen for bipolarons in CPs.

The spectroelectrochemistry of polymers typically shows two transitions representing the polaron to bipolaron transition. Interestingly, oxidized P1 does not exhibit the most far red-shifted absorption in the nPB series. Oxidation from the polaron to bipolaron state results in a hypsochromic shift from 1.23/0.73 to 0.86 eV. This hypsochromic shift of the bipolaron species can be rationalized by stronger lattice deformations of two positive charges in comparison to one positive charge, thereby causing the mid-gap transition to be further away from the band edge and requiring higher-energy electronic transitions. 107 However, the DNPV of P1 shows six small peaks before the large peak at 1.9 V (Figure S6 in the Supporting Information) in a voltammetry pattern similar to the voltammograms of 9, 15, and 21. There are approximately seven anodic peaks for P1, making it reasonable to assume that the very broad optical absorption bands of doped P1 are due to the formation of diverse species within the chain and not just mere polaron-bipolaron charges. Indeed, TDDFT calculations for the polaron, bipolaron, and di-polaron states of 5, 7, and 9 reveal that these bands have several peaks in the same energetic area, suggesting that deconvolution of the spectra could be difficult.

CONCLUSIONS

In summary, we describe herein the molecular structure, chain conformation, and oxidation states of a series of monodisperse and discrete molecules composed of ProDOT-BTD D–A monomers with small molecule to polymer length scales. These results reflect the impact of the chain length on the conformation and oxidation behavior of π -conjugated, weakly interacting, D–A oligomers and polymers in the solution state, which is important for solution-processed CP thin films. We demonstrated the following findings in this study:

- **1. Chain Conformations.** The neutral backbone conformation undergoes a rod-to-coil transition at **15**-unit chain length, revealing that oligomers shorter than **15** units exist as semirigid, worm-like chains in solution with an $L_{\rm p}$ up to 2.5 nm, while longer chains begin to coil. The longest polymer **P3** (~43 units) has a persistence length of 3.1 nm, proving that elongation of the polymer chain does not necessarily improve the conjugation length.
- 2. Oxidation States. In their dication states, short, semirigid chains prefer bipolaron formation, while the long coil-like oligomers prefer di-polaron formation. This result is verified by DFT and is experimentally proven by voltammetry, as the ΔE (Coulombic repulsion) between the first and second oxidation steps increases from 3 to 9 and decreases at longer lengths due to chain coiling. The rod-to-coil transition is emulated during electrochemical oxidation as the voltammetric response changes from a single-electron transfer per step to multielectron-transfer per step at n = 15. The polymer voltammogram reveals similar anodic wave patterns to n =9-21, implying that there are multioxidation states in CPs instead of just "polarons and bipolarons". Additionally, the continuous decrease in the oxidation potential after a maximum conjugation length has been reached highlights the gaps in understanding the role of chain conformation, solution interactions, and ions in the redox reaction of CPs, warranting further studies.
- **3. Optical Properties.** The lowest energy electronic transition of the +1 state undergoes a bathochromic shift from 3 to 15 units and reverses to a hypsochromic shift at longer lengths. This is the same trend observed for the +2 state for the *n*PB series. The dication state of 15 absorbs further in the NIR region than the polymer in solution, with no major change or enhancement in optical properties with an increase in the doping level or chain length. This result reveals the cooperation between the chain length and the oxidation state, showing that the increase in the chain length can also have an adverse effect on optical properties depending on application needs

This detailed and systematic investigation of the length-dependent chain structure and optoelectronic properties for a D-A, ProDOT-BTD-based oligomer and polymer series will further guide the rational design and prediction of future CPs for application in organic electronics.

■ EXPERIMENTAL METHODS

I

SANS Measurements. Dilute solutions of oligomers and polymers were prepared (5 mg/mL) in chlorobenzene-d5. Chlorobenzene-d5 (D > 99%) was purchased from Cambridge Isotope Laboratories (Tewksbury, MA) and used as received. SANS measurements were carried out using the extended Q-range smallangle neutron scattering diffractometer at the Spallation Neutron Source (SNS), ORNL. The scattering wavevector q ranged from 0.003 to 0.8 Å $^{-1}$, by using two different configurations (4 m 12 Å and

2.5~m 2.5~Å). The samples were contained in Hellma quartz cells with a 2 mm path length. Measurements were performed at 75 °C. The absolute intensity was obtained through data reduction and correction. The reduced data were later fitted to a flexible cylinder model in SasView.

Voltammetry. Solution CV and DPV was performed on ~ 1 mM samples in 0.2 M TBAPF₆/CH₂Cl₂ under a nitrogen atmosphere using a UME (25 μ m) Pt wire electrode and a Pt wire counter electrode. An Ag/AgCl wire was used as the pseudoreference electrode which was calibrated against ferrocene/ferrocenium as an internal standard ($E_{1/2} = 0.51$ V). The voltage was scanned from 0 to 2.0 V *versus* Ag/AgCl, at a 10 mV/s scan rate. The second cycle is reported. The electrochemical window of the electrolyte system was found to be stable up to 2.1 V and began to degrade at 2.2 V, as shown in Supporting Information, Figure S4.

Spectroelectrochemistry. Solution spectroelectrochemistry was done in a three-electrode honeycomb electrochemical cell supplied by Pine Research. A 12.5 \times 12.5 \times 45.0 mm³ quartz cuvette with a 1.7 mm path length was used as the cell, equipped with a polished Pt honeycomb electrode (working and counter) and a Ag/AgCl pseudoreference electrode calibrated against a ferrocene/ferrocenium standard for which the $E_{1/2}$ is taken to be 0.51 V *versus* Ag/AgCl. A homemade Teflon cap was specially designed to keep the cell sealed from solvent evaporation and air contamination. In a nitrogen-filled glovebox, 4×10^{-4} M solution of the analyte was prepared with 0.2 M TBAPF₆ in anhydrous DCM, transferred to the electrochemical quartz cell, and sealed with Teflon tape. During electrochemical oxidation, the voltage increased from 0 to 2.0 V in ~25 mV increments by linear scan voltammetry at a 25 mV/s scan rate.

ASSOCIATED CONTENT

Supporting Information

The Supporting Information is available free of charge at https://pubs.acs.org/doi/10.1021/acs.macromol.1c00963.

Experimental and characterization data; synthetic procedure and purification of oligomers and polymers; raw GPC data; raw and deconvoluted CV and DPV curves; AFM image of a five-unit oligomer; raw SANS data; DFT and TDDFT calculations; and NMR spectra (PDF)

AUTHOR INFORMATION

Corresponding Authors

Chad Risko – Department of Chemistry & Center for Applied Energy Research (CAER), University of Kentucky, Lexington, Kentucky 40506, United States; orcid.org/0000-0001-9838-5233; Email: chad.risko@uky.edu

Jianguo Mei — Department of Chemistry, Purdue University, West Lafayette, Indiana 47907, United States; oocid.org/0000-0002-5743-2715; Email: jgmei@purdue.edu

Authors

Saadia Chaudhry – Department of Chemistry, Purdue University, West Lafayette, Indiana 47907, United States

Yukun Wu – Department of Chemistry, Purdue University, West Lafayette, Indiana 47907, United States

Zhiqiang Cao – School of Polymer Science and Engineering, The University of Southern Mississippi, Hattiesburg, Mississippi 39406, United States

Shi Li – Department of Chemistry & Center for Applied Energy Research (CAER), University of Kentucky, Lexington, Kentucky 40506, United States

Jodie L. Canada – Department of Chemistry & Center for Applied Energy Research (CAER), University of Kentucky, Lexington, Kentucky 40506, United States Xiaodan Gu — School of Polymer Science and Engineering, The University of Southern Mississippi, Hattiesburg, Mississippi 39406, United States; orcid.org/0000-0002-1123-3673

Complete contact information is available at: https://pubs.acs.org/10.1021/acs.macromol.1c00963

Notes

The authors declare no competing financial interest.

ACKNOWLEDGMENTS

S.C., Y.W., and J.M. acknowledge the Bilsland Dissertation Fellowship and the Office of Naval Research through the Energetic Materials Program (MURI grant no: N00014-21-1-2476, Program Manager: Dr. Chad Stoltz). S.L., J.C., and C.R. acknowledge the Office of Naval Research Young Investigator Program (award no. N00014-18-1-2448; chain-length-dependent electronic and optical property studies) and the NSF (award no. DMR-1905734; method benchmarking and analyses of polaron, bipolaron, and di-polaron formation). Supercomputing resources on the Lipscomb High-Performance Computing Cluster were provided by the University of Kentucky Information Technology Department and the Center for Computational Sciences (CCS). Z.C. and X.G. thank the U.S. Department of Energy, Office of Science, Office of Basic Energy Science under award number DE-SC0019361 for supporting the neutron scattering study in this work. Part of the research used resources at the Spallation Neutron Source, DOE Office of Science User Facilities operated by the Oak Ridge National Laboratory.

REFERENCES

- (1) Kuei, B.; Gomez, E. D. Chain Conformations and Phase Behavior of Conjugated Polymers. *Soft Matter* **2017**, *13*, 49–67.
- (2) Lüssem, B.; Keum, C.-M.; Kasemann, D.; Naab, B.; Bao, Z.; Leo, K. Doped Organic Transistors. *Chem. Rev.* **2016**, *116*, 13714–13751.
- (3) Beaujuge, P. M.; Ellinger, S.; Reynolds, J. R. The Donor-Acceptor Approach Allows Ablack-to-Transmissive Switching Polymeric Electrochrome. *Nat. Mater.* **2008**, *7*, 795–799.
- (4) Beaujuge, P. M.; Reynolds, J. R. Color Control in π -Conjugated Organic Polymers for Use in Electrochromic Devices. *Chem. Rev.* **2010**, *110*, 268–320.
- (5) Teran, N. B.; Reynolds, J. R. Discrete Donor-Acceptor Conjugated Systems in Neutral and Oxidized States: Implications toward Molecular Design for High Contrast Electrochromics. *Chem. Mater.* **2017**, 29, 1290–1301.
- (6) Groenendaal, L.; Zotti, G.; Aubert, P.-H.; Waybright, S. M.; Reynolds, J. R. Electrochemistry of Poly(3,4-Alkylenedioxythiophene) Derivatives. *Adv. Mater.* **2003**, *15*, 855–879.
- (7) Beaujuge, P. M.; Vasilyeva, S. V.; Liu, D. Y.; Ellinger, S.; McCarley, T. D.; Reynolds, J. R. Structure-Performance Correlations in Spray-Processable Green Dioxythiophene-Benzothiadiazole Donor-Acceptor Polymer Electrochromes. *Chem. Mater.* **2012**, *24*, 255–268.
- (8) Groenendaal, L.; Jonas, F.; Freitag, D.; Pielartzik, H.; Reynolds, J. R. Poly(3,4-Ethylenedioxythiophene) and Its Derivatives: Past, Present, and Future. *Adv. Mater.* **2000**, *12*, 481–494.
- (9) Shi, P.; Amb, C. M.; Knott, E. P.; Thompson, E. J.; Liu, D. Y.; Mei, J.; Dyer, A. L.; Reynolds, J. R. Broadly Absorbing Black to Transmissive Switching Electrochromic Polymers. *Adv. Mater.* **2010**, 22, 4949–4953.
- (10) Sekine, C.; Tsubata, Y.; Yamada, T.; Kitano, M.; Doi, S. Recent Progress of High Performance Polymer OLED and OPV Materials for Organic Printed Electronics. *Sci. Technol. Adv. Mater.* **2014**, *15*, 034203.
- (11) Winsberg, J.; Hagemann, T.; Muench, S.; Friebe, C.; Häupler, B.; Janoschka, T.; Morgenstern, S.; Hager, M. D.; Schubert, U. S.

- Poly(Boron-Dipyrromethene)-A Redox-Active Polymer Class for Polymer Redox-Flow Batteries. *Chem. Mater.* **2016**, 28, 3401–3405.
- (12) Oh, S. H.; Lee, C.-W.; Chun, D. H.; Jeon, J.-D.; Shim, J.; Shin, K. H.; Yang, J. H. A Metal-Free and All-Organic Redox Flow Battery with Polythiophene as the Electroactive Species. *J. Mater. Chem. A* **2014**, *2*, 19994–19998.
- (13) Nagarjuna, G.; Hui, J.; Cheng, K. J.; Lichtenstein, T.; Shen, M.; Moore, J. S.; Rodríguez-López, J. Impact of Redox-Active Polymer Molecular Weight on the Electrochemical Properties and Transport across Porous Separators in Nonaqueous Solvents. *J. Am. Chem. Soc.* **2014**, *136*, 16309–16316.
- (14) Montoto, E. C.; Nagarjuna, G.; Hui, J.; Burgess, M.; Sekerak, N. M.; Hernández-Burgos, K.; Wei, T.-S.; Kneer, M.; Grolman, J.; Cheng, K. J.; et al. Redox Active Colloids as Discrete Energy Storage Carriers. J. Am. Chem. Soc. 2016, 138, 13230–13237.
- (15) Xie, J.; Gu, P.; Zhang, Q. Nanostructured Conjugated Polymers: Toward High-Performance Organic Electrodes for Rechargeable Batteries. ACS Energy Lett. 2017, 2, 1985–1996.
- (16) Mei, J.; Graham, K. R.; Stalder, R.; Tiwari, S. P.; Cheun, H.; Shim, J.; Yoshio, M.; Nuckolls, C.; Kippelen, B.; Castellano, R. K.; et al. Self-Assembled Amphiphilic Diketopyrrolopyrrole-Based Oligothiophenes for Field-Effect Transistors and Solar Cells. *Chem. Mater.* **2011**, 23, 2285–2288.
- (17) McQuade, D. T.; Pullen, A. E.; Swager, T. M. Conjugated Polymer-Based Chemical Sensors. *Chem. Rev.* **2000**, *100*, 2537–2574.
- (18) Wang, J.; Lv, F.; Liu, L.; Ma, Y.; Wang, S. Strategies to Design Conjugated Polymer Based Materials for Biological Sensing and Imaging. *Coord. Chem. Rev.* **2018**, 354, 135–154.
- (19) Van Mullekom, H. A. M.; Vekemans, J. A. J. M.; Havinga, E. E.; Meijer, E. W. Developments in the Chemistry and Band Gap Engineering of Donor-Acceptor Substituted Conjugated Polymers. *Mater. Sci. Eng., R* **2001**, *32*, 1.
- (20) Zhou, C.; Liang, Y.; Liu, F.; Sun, C.; Huang, X.; Xie, Z.; Huang, F.; Roncali, J.; Russell, T. P.; Cao, Y. Chain Length Dependence of the Photovoltaic Properties of Monodisperse Donor-Acceptor Oligomers as Model Compounds of Polydisperse Low Band Gap Polymers. *Adv. Funct. Mater.* **2014**, *24*, 7538–7547.
- (21) Fauvell, T. J.; Zheng, T.; Jackson, N. E.; Ratner, M. A.; Yu, L.; Chen, L. X. Photophysical and Morphological Implications of Single-Strand Conjugated Polymer Folding in Solution. *Chem. Mater.* **2016**, 28, 2814–2822.
- (22) Wang, Z.-G. 50th Anniversary Perspective: Polymer Conformation-A Pedagogical Review. *Macromolecules* **2017**, *50*, 9073–9114.
- (23) Lu, Y.; Weers, B.; Stellwagen, N. C. DNA Persistence Length Revisited. *Biopolymers* **2002**, *61*, 261–275.
- (24) Gross, P.; Laurens, N.; Oddershede, L. B.; Bockelmann, U.; Peterman, E. J. G.; Wuite, G. J. L. Quantifying How DNA Stretches, Melts and Changes Twist under Tension. *Nat. Phys.* **2011**, *7*, 731–736.
- (25) Roux, C.; Leclerc, M. Rod-to-Coil Transition in Alkoxy-Substituted Polythiophenes. *Macromolecules* **1992**, *25*, 2141–2144.
- (26) Mattice, W. L.; Suter, U. W. Conformational Theory of Large Molecules: The Rotational Isomeric State Model in Macromolecular Systems; Wiley, 1994.
- (27) McCulloch, B.; Ho, V.; Hoarfrost, M.; Stanley, C.; Do, C.; Heller, W. T.; Segalman, R. A. Polymer Chain Shape of Poly(3-Alkylthiophenes) in Solution Using Small-Angle Neutron Scattering. *Macromolecules* **2013**, *46*, 1899–1907.
- (28) Gu, K.; Loo, Y. L. The Polymer Physics of Multiscale Charge Transport in Conjugated Systems. *J. Polym. Sci., Part B: Polym. Phys.* **2019**, *57*, 1559–1571.
- (29) Mao, H.; Xu, B.; Holdcroft, S. Synthesis and Structure—Property Relationships of Regioirregular Poly(3-Hexylthiophenes). *Macromolecules* **1993**, *26*, 1163–1169.
- (30) Cao, Z.; Li, Z.; Zhang, S.; Galuska, L.; Li, T.; Do, C.; Xia, W.; Hong, K.; Gu, X. Decoupling Poly(3-Alkylthiophenes)' Backbone and Side-Chain Conformation by Selective Deuteration and Neutron Scattering. *Macromolecules* **2020**, *53*, 11142–11152.

- (31) Brinkmann, M.; Wittmann, J.-C. Orientation of Regioregular Poly(3-Hexylthiophene) by Directional Solidification: A Simple Method to Reveal the Semicrystalline Structure of a Conjugated Polymer. *Adv. Mater.* **2006**, *18*, 860–863.
- (32) Brinkmann, M. Structure and Morphology Control in Thin Films of Regioregular Poly(3-Hexylthiophene). J. Polym. Sci., Part B: Polym. Phys. **2011**, 49, 1218–1233.
- (33) Trznadel, M.; Pron, A.; Zagorska, M.; Chrzaszcz, R.; Pielichowski, J. Effect of Molecular Weight on Spectroscopic and Spectroelectrochemical Properties of Regioregular Poly(3-Hexylthiophene). *Macromolecules* **1998**, *31*, 5051–5058.
- (34) Kayunkid, N.; Uttiya, S.; Brinkmann, M. Structural Model of Regioregular Poly(3-Hexylthiophene) Obtained by Electron Diffraction Analysis. *Macromolecules* **2010**, *43*, 4961–4967.
- (35) Kline, R. J.; McGehee, M. D.; Kadnikova, E. N.; Liu, J.; Fréchet, J. M. J.; Toney, M. F. Dependence of Regioregular Poly(3-Hexylthiophene) Film Morphology and Field-Effect Mobility on Molecular Weight. *Macromolecules* **2005**, *38*, 3312–3319.
- (36) Yamamoto, J.; Furukawa, Y. Electronic and Vibrational Spectra of Positive Polarons and Bipolarons in Regioregular Poly(3-Hexylthiophene) Doped with Ferric Chloride. *J. Phys. Chem. B* **2015**, *119*, 4788–4794.
- (37) Kim, Y.; Cook, S.; Choulis, S. A.; Nelson, J.; Durrant, J. R.; Bradley, D. D. C. Organic Photovoltaic Devices Based on Blends of Regioregular Poly(3-Hexylthiophene) and Poly(9,9-Dioctylfluorene-Co-Benzothiadiazole). *Chem. Mater.* **2004**, *16*, 4812–4818.
- (38) Wang, G.; Swensen, J.; Moses, D.; Heeger, A. J. Increased Mobility from Regioregular Poly(3-Hexylthiophene) Field-Effect Transistors. *J. Appl. Phys.* **2003**, 93, 6137–6141.
- (39) Kim, Y.; Choulis, S. A.; Nelson, J.; Bradley, D. D. C.; Cook, S.; Durrant, J. R. Device Annealing Effect in Organic Solar Cells with Blends of Regioregular Poly(3-Hexylthiophene) and Soluble Fullerene. *Appl. Phys. Lett.* **2005**, *86*, 63502.
- (40) Bao, Z.; Dodabalapur, A.; Lovinger, A. J. Soluble and Processable Regioregular Poly(3-Hexylthiophene) for Thin Film Field-Effect Transistor Applications with High Mobility. *Appl. Phys. Lett.* **1996**, *69*, 4108–4110.
- (41) Electronic Materials: The Oligomer Approach; Müllen, K., Wegner, G., Eds.; Wiley-VCH Verlag GmbH: Weinheim, Germany, 1998.
- (42) Heinze, J. x. r.; Tschuncky, P.; Smie, A. The Oligomeric Approach The Electrochemistry of Conducting Polymers in the Light of Recent Research. *J. Solid State Electrochem.* 1998, 2, 102–109.
- (43) Tour, J. M. Conjugated Macromolecules of Precise Length and Constitution. Organic Synthesis for the Construction of Nanoarchitectures. *Chem. Rev.* **1996**, *96*, 537–554.
- (44) Martin, R. E.; Diederich, F. Linear Monodisperse π -Conjugated Oligomers: Model Compounds for Polymers and More. *Angew. Chem. Int. Ed.* **1999**, 38, 1350–1377.
- (45) Meerholz, K.; Heinze, J. Electrochemical Solution and Solid-State Investigations on Conjugated Oligomers and Polymers of the α -Thiophene and the p-Phenylene Series. *Electrochim. Acta* **1996**, 41, 1839–1854.
- (46) Heinze, J.; Tschuncky, P. Electrochemical Properties. *Electronic Materials: The Oligomer Approach*, Wiley, 2007; pp 480–514.
- (47) Heinze, J.; Frontana-Uribe, B. A.; Ludwigs, S. Electrochemistry of Conducting Polymers-Persistent Models and New Concepts. *Chem. Rev.* **2010**, *110*, 4724–4771.
- (48) van Haare, J. A. E. H.; Havinga, E. E.; van Dongen, J. L. J.; Janssen, R. A. J.; Cornil, J.; Brédas, J.-L.; Van Haare, J. A. E. H.; Havinga, E. E.; Van Dongen, J. L. J.; Janssen, R. A. J. J.; et al. Redox States of Long Oligothiophenes: Two Polarons on a Single Chain. *Chem.—Eur. J.* 1998, 4, 1509–1522.
- (49) Fichou, D.; Horowitz, G.; Garnier, F. Polaron and Bipolaron Formation on Isolated Model Thiophene Oligomers in Solution. *Synth. Met.* **1990**, *39*, 125–131.

- (50) Zade, S. S.; Zamoshchik, N.; Bendikov, M. From Short Conjugated Oligomers to Conjugated Polymers. Lessons from Studies on Long Conjugated Oligomers. *Acc. Chem. Res.* **2011**, *44*, 14–24.
- (51) Fichou, D.; Xu, B.; Horowitz, G.; Garnier, F. Generation of Stabilized Polarons and Bipolarons on Extended Model Thiophene Oligomers. *Synth. Met.* **1991**, *41*, 463–469.
- (52) Zaikowski, L.; Kaur, P.; Gelfond, C.; Selvaggio, E.; Asaoka, S.; Wu, Q.; Chen, H.-C.; Takeda, N.; Cook, A. R.; Yang, A.; et al. Polarons, Bipolarons, and Side-by-Side Polarons in Reduction of Oligofluorenes. *J. Am. Chem. Soc.* **2012**, *134*, 10852–10863.
- (\tilde{S} 3) Van Haare, J. A. E. H.; Van Boxtel, M.; Janssen, R. A. J. π -Dimers of Prototype High-Spin Polaronic Oligomers. *Chem. Mater.* **1998**, *10*, 1166–1175.
- (54) Van Haare, J. A. E. H.; Havinga, E. E.; Van Dongen, J. L. J.; Janssen, R. A. J.; Cornil, J.; Brédas, J.-L. Redox States of Long Oligothiophenes: Two Polarons on a Single Chain. *Chem.—Eur. J.* 1998, 4, 1509–1522.
- (55) Cao, J.; Curtis, M. D. Polarons, Bipolarons, and π -Dimers of Bis(3,4-Ethylene-Dioxythiophene)-(4,4'-Dialkyl-2,2'-Bithiazole) -Co-Oligomers. Direct Measure of the Intermolecular Exciton Transfer Interaction. *Chem. Mater.* **2003**, *15*, 4424–4430.
- (56) Lacroix, J. C.; Chane-Ching, K. I.; Maquère, F.; Maurel, F. Intrachain Electron Transfer in Conducting Oligomers and Polymers: The Mixed Valence Approach. *J. Am. Chem. Soc.* **2006**, *128*, 7264–7276.
- (57) He, J.; Crase, J. L.; Wadumethrige, S. H.; Thakur, K.; Dai, L.; Zou, S.; Rathore, R.; Hartley, C. S. Ortho-Phenylenes: Unusual Conjugated Oligomers with a Surprisingly Long Effective Conjugation Length. *J. Am. Chem. Soc.* **2010**, *132*, 13848–13857.
- (58) Izumi, T.; Kobashi, S.; Takimiya, K.; Aso, Y.; Otsubo, T. Synthesis and Spectroscopic Properties of a Series of β -Blocked Long Oligothiophenes up to the 96-Mer: Revaluation of Effective Conjugation Length. *J. Am. Chem. Soc.* **2003**, *125*, 5286–5287.
- (59) Gaylord, B. S.; Wang, S.; Heeger, A. J.; Bazan, G. C. Water-Soluble Conjugated Oligomers: Effect of Chain Length and Aggregation on Photoluminescence-Quenching Efficiencies. *J. Am. Chem. Soc.* **2001**, 123, 6417–6418.
- (60) Zade, S. S.; Bendikov, M. From Oligomers to Polymer: Convergence in the HOMO-LUMO Gaps of Conjugated Oligomers. *Org. Lett.* **2006**, *8*, 5243–5246.
- (61) Grimme, J.; Kreyenschmidt, M.; Uckert, F.; Müllen, K.; Scherf, U. On the Conjugation Length in Poly(Para-phenylene)-type Polymers. *Adv. Mater.* **1995**, *7*, 292–295.
- (62) Klaerner, G.; Miller, R. D. Polyfluorene Derivatives: Effective Conjugation Lengths from Well-Defined Oligomers. *Macromolecules* **1998**, *31*, 2007–2009.
- (63) Meier, H.; Stalmach, U.; Kolshorn, H. Effective Conjugation Length and UV/Vis Spectra of Oligomers. *Acta Polym.* 1997, 48, 379–384
- (64) Bäuerle, P. End-capped Oligothiophenes—New Model Compounds for Polythiophenes. *Adv. Mater.* **1992**, *4*, 102–107.
- (65) Wasserberg, D.; Meskers, S. C. J.; Janssen, R. A. J.; Mena-Osteritz, E.; Bäuerle, P. High-Resolution Electronic Spectra of Ethylenedioxythiophene Oligomers. *J. Am. Chem. Soc.* **2006**, *128*, 17007–17017.
- (66) Fitzner, R.; Reinold, E.; Mishra, A.; Mena-Osteritz, E.; Ziehlke, H.; Körner, C.; Leo, K.; Riede, M.; Weil, M.; Tsaryova, O.; et al. Dicyanovinyl-Substituted Oligothiophenes: Structure-Property Relationships and Application in Vacuum-Processed Small Molecule Organic Solar Cells. *Adv. Funct. Mater.* **2011**, *21*, 897–910.
- (67) Bäuerle, P.; Fischer, T.; Bidlingmeier, B.; Rabe, J. P.; Stabel, A. Oligothiophenes—Yet Longer? Synthesis, Characterization, and Scanning Tunneling Microscopy Images of Homologous, Isomerically Pure Oligo(Alkylthiophene)S. *Angew Chem. Int. Ed. Engl.* 1995, 34, 303–307.
- (68) Kim, T.-W.; Kim, W.; Park, K. H.; Kim, P.; Cho, J.-W.; Shimizu, H.; Iyoda, M.; Kim, D. Chain-Length-Dependent Exciton Dynamics in Linear Oligothiophenes Probed Using Ensemble and Single-Molecule Spectroscopy. *J. Phys. Chem. Lett.* **2016**, *7*, 452–458.

- (69) Roncali, J.; Blanchard, P.; Frère, P. 3,4-Ethylenedioxythiophene (EDOT) as a Versatile Building Block for Advanced Functional π -Conjugated Systems. *J. Mater. Chem.* **2005**, *15*, 1589–1610.
- (70) Turbiez, M.; Frère, P.; Allain, M.; Videlot, C.; Ackermann, J.; Roncali, J. Design of Organic Semiconductors: Tuning the Electronic Properties of π -Conjugated Oligothiophenes with the 3,4-Ethylenedioxythiophene (EDOT) Building Block. *Chem.—Eur. J.* **2005**, *11*, 3742–3752.
- (71) Baeuerle, P.; Segelbacher, U.; Maier, A.; Mehring, M. Electronic Structure of Mono- and Dimeric Cation Radicals in End-Capped Oligothiophenes. *J. Am. Chem. Soc.* **1993**, *115*, 10217–10223.
- (72) Mathew, S. M.; Hartley, C. S. Parent O-Phenylene Oligomers: Synthesis, Conformational Behavior, and Characterization. *Macromolecules* **2011**, *44*, 8425–8432.
- (73) Sharber, S. A.; Baral, R. N.; Frausto, F.; Haas, T. E.; Müller, P.; Thomas, S. W. Substituent Effects That Control Conjugated Oligomer Conformation through Non-Covalent Interactions. *J. Am. Chem. Soc.* **2017**, *139*, 5164–5174.
- (74) Stone, M. T.; Heemstra, J. M.; Moore, J. S. The Chain-Length Dependence Test. *Acc. Chem. Res.* **2006**, *39*, 11–20.
- (75) Nguyen, T.-Q.; Doan, V.; Schwartz, B. J. Conjugated Polymer Aggregates in Solution: Control of Interchain Interactions. *J. Chem. Phys.* **1999**, *110*, 4068–4078.
- (76) Roncali, J. Oligothienylenevinylenes as a New Class of Multinanometer Linear π Conjugated Systems for Micro- and Nanoelectronics. *Acc. Chem. Res.* **2000**, 33, 147–156.
- (77) Martin, R. E.; Gubler, U.; Cornil, J.; Balakina, M.; Boudon, C.; Bosshard, C.; Gisselbrecht, J.-P.; Diederich, F.; Günter, P.; Gross, M.; et al. Monodisperse Poly(Triacetylene) Oligomers Extending from Monomer to Hexadecamer: Joint Experimental and Theoretical Investigation of Physical Properties. *Chem.—Eur. J.* **2000**, *6*, 3622–3635.
- (78) Martin, R. E.; Günter, P.; Bosshard, C.; Gubler, U.; Gramlich, V.; Gross, M.; Boudon, C.; Gisselbrecht, J.-P.; Diederich, F. Poly(Triacetylene) Oligomers: Synthesis, Characterization, and Estimation of the Effective Conjugation Length by Electrochemical, UV/Vis, and Nonlinear Optical Methods. *Chem.—Eur. J.* 1997, 3, 1505–1512.
- (79) Bücker, D.; Sickinger, A.; Ruiz Perez, J. D.; Oestringer, M.; Mecking, S.; Drescher, M. Direct Observation of Chain Lengths and Conformations in Oligofluorene Distributions from Controlled Polymerization by Double Electron-Electron Resonance. *J. Am. Chem. Soc.* **2020**, *142*, 1952–1956.
- (80) Liu, Q.; Liu, W.; Yao, B.; Tian, H.; Xie, Z.; Geng, Y.; Wang, F. Synthesis and Chain-Length Dependent Properties of Monodisperse Oligo(9,9-Di-n-Octylfluorene-2,7-Vinylene)S. *Macromolecules* **2007**, 40, 1851–1857.
- (81) Yu, H.; Li, S.; Schwieter, K. E.; Liu, Y.; Sun, B.; Moore, J. S.; Schroeder, C. M. Charge Transport in Sequence-Defined Conjugated Oligomers. *J. Am. Chem. Soc.* **2020**, *142*, 4852–4861.
- (82) Ellinger, S.; Graham, K. R.; Shi, P.; Farley, R. T.; Steckler, T. T.; Brookins, R. N.; Taranekar, P.; Mei, J.; Padilha, L. A.; Ensley, T. R.; et al. Donor-Acceptor-Donor-Based π -Conjugated Oligomers for Nonlinear Optics and near-IR Emission. *Chem. Mater.* **2011**, 23, 3805–3817.
- (83) Liu, J.; Li, L.; Xu, R.; Zhang, K.; Ouyang, M.; Li, W.; Lv, X.; Zhang, C. Design, Synthesis, and Properties of Donor–Acceptor–Donor' Asymmetric Structured Electrochromic Polymers Based on Fluorenone as Acceptor Units. *ACS Appl. Polym. Mater.* **2019**, *1*, 1081–1087.
- (84) Pluczyk-Malek, S.; Honisz, D.; Akkuratov, A.; Troshin, P.; Lapkowski, M. Tuning the Electrochemical and Optical Properties of Donor-Acceptor D-A2-A1-A2-D Derivatives with Central Benzothia-diazole Core by Changing the A2 Strength. *Electrochim. Acta* **2021**, 368, 137540.
- (85) Xia, H.; Xu, X.; Guo, J.; Qian, C.; Zhang, K.; Zhu, M.; Zhang, B.; Peng, W.; Peng, Q.; Zhu, W. Structure Evolution from D-A-D Type Small Molecule toward D-A-D-A-D Type Oligomer for High-

- Efficiency Photovoltaic Donor Materials. Dyes Pigm. 2021, 186, 108950.
- (86) Karsten, B. P.; Bijleveld, J. C.; Viani, L.; Cornil, J.; Gierschner, J.; Janssen, R. A. J. Electronic Structure of Small Band Gap Oligomers Based on Cyclopentadithiophenes and Acceptor Units. *J. Mater. Chem.* **2009**, *19*, 5343–5350.
- (87) Chai, J.-D.; Head-Gordon, M. Long-Range Corrected Hybrid Density Functionals with Damped Atom-Atom Dispersion Corrections. *Phys. Chem. Chem. Phys.* **2008**, *10*, 6615–6620.
- (88) Francl, M. M.; Pietro, W. J.; Hehre, W. J.; Binkley, J. S.; Gordon, M. S.; DeFrees, D. J.; Pople, J. A. Self-Consistent Molecular Orbital Methods. XXIII. A Polarization-Type Basis Set for Second-Row Elements. J. Chem. Phys. 1982, 77, 3654–3665.
- (89) Hariharan, P. C.; Pople, J. A. The Influence of Polarization Functions on Molecular Orbital Hydrogenation Energies. *Theor. Chim. Acta* 1973, 28, 213–222.
- (90) Stein, T.; Eisenberg, H.; Kronik, L.; Baer, R. Fundamental Gaps in Finite Systems from Eigenvalues of a Generalized Kohn-Sham Method. *Phys. Rev. Lett.* **2010**, *105*, 266802.
- (91) Refaely-Abramson, S.; Baer, R.; Kronik, L. Fundamental and Excitation Gaps in Molecules of Relevance for Organic Photovoltaics from an Optimally Tuned Range-Separated Hybrid Functional. *Phys. Rev. B: Condens. Matter Mater. Phys.* **2011**, 84, 075144.
- (92) Stein, T.; Kronik, L.; Baer, R. Reliable Prediction of Charge Transfer Excitations in Molecular Complexes using Time-Dependent Density Functional Theory. *J. Am. Chem. Soc.* **2009**, *131*, 2818–2820.
- (93) Frisch, M. J. .; Trucks, G. W. .; Schlegel, H. B. .; Scuseria, G. E. .; Robb, M. A. .; Cheeseman, J. R. .; Scalmani, G. .; Barone, V. .; Mennucci, B. .; Petersson, G. A. .; et al. *Gaussian 09 Citationl Gaussian.Com*, 2009.
- (94) Risko, C.; McGehee, M. D.; Brédas, J.-L. A Quantum-Chemical Perspective into Low Optical-Gap Polymers for Highly-Efficient Organic Solar Cells. *Chem. Sci.* **2011**, *2*, 1200–1218.
- (95) Gierschner, J.; Cornil, J.; Egelhaaf, H.-J. Optical Bandgaps of π -Conjugated Organic Materials at the Polymer Limit: Experiment and Theory. *Adv. Mater.* **2007**, *19*, 173–191.
- (96) Rissler, J. Effective Conjugation Length of π -Conjugated Systems. *Chem. Phys. Lett.* **2004**, 395, 92–96.
- (97) Kuhn, H. A Quantum-Mechanical Theory of Light Absorption of Organic Dyes and Similar Compounds. *J. Chem. Phys.* **1949**, *17*, 1198–1212.
- (98) Robin, M. B.; Day, P. Mixed Valence Chemistry-A Survey and Classification. *Adv. Inorg. Chem. Radiochem.* **1968**, *10*, 247–422.
- (99) Heinze, J. Ultramicroelectrodes in Electrochemistry. *Angew Chem. Int. Ed. Engl.* **1993**, 32, 1268–1288.
- (100) Wightman, R. M.; Wipf, D. Electroanalytical Chemistry; Bard, A., Ed.; Marcal Dekker: New York, 1989.
- (101) Aoki, K. Theory of Ultramicroelectrodes. *Electroanalysis* **1993**, 5, 627–639.
- (102) Chaudhry, S.; Ryno, S. M.; Zeller, M.; McMillin, D. R.; Risko, C.; Mei, J. Oxidation Pathways Involving a Sulfide-Endcapped Donor-Acceptor-Donor π -Conjugated Molecule and Antimony(V) Chloride. *J. Phys. Chem. B* **2019**, 123, 3866–3874.
- (103) Qin, R.; Bo, Z. Synthesis and Characterization of 2,7-Linked Carbazole Oligomers. *Macromol. Rapid Commun.* **2012**, 33, 87–91.
- (104) Vacareanu, L.; Grigoras, M. Electrochemical Characterization of Arylene Vinylene Oligomers Containing Triphenylamine and Carbazole Units. *J. Appl. Electrochem.* **2010**, *40*, 1967–1975.
- (105) Chen, H. C.; Sreearunothai, P.; Cook, A. R.; Asaoka, S.; Wu, Q.; Miller, J. R. Chain Length Dependence of Energies of Electron and Triplet Polarons in Oligofluorenes. *J. Phys. Chem. C* **2017**, *121*, 5959–5967.
- (106) Heimel, G. The Optical Signature of Charges in Conjugated Polymers. ACS Cent. Sci. 2016, 2, 309–315.
- (107) Brédas, J. L.; Street, G. B. Polarons, Bipolarons, and Solitons in Conducting Polymers. Acc. Chem. Res. 1985, 18, 309-315.